White Dwarfs as Probes of Fundamental Physics: Tracers of Planetary, Stellar and Galactic Evolution
Proceedings IAU Symposium No. 357, 2019
M. A. Barstow, S. J. Kleinman, J. L. Provencal & L. Ferrario, eds.
doi:10.1017/S1743921320000617

(Pre)-white dwarf stars as measuring tools for yields of AGB nucleosynthesis

Lisa Löbling

Institut für Astronomie und Astrophysik, Sand 1, 72076 Tübingen, Germany
email: loebling@astro.uni-tuebingen.de

Abstract. In the helium-rich intershell region of asymptotic giant branch (AGB) stars, slow neutron-capture nucleosynthesis produces heavy elements beyond iron. If the stars experience a final-flash of the He-burning shell, a pulse-driven convection zone establishes, the stars become hydrogen-deficient and exhibit former intershell material at their surfaces. In their subsequent evolution towards the white-dwarf cooling sequence, but still at constant luminosity, a strong stellar wind prevents diffusion to wipe out the information about AGB yields. We present and interpret the analysis results of hydrogen-rich and -deficient post-AGB stars, discuss difficulties in their analysis and review the implications on the understanding of post-AGB evolution.

Keywords. atomic data, techniques: spectroscopic, stars: abundances, stars: AGB and post-AGB, stars: atmospheres, white dwarfs, planetary nebulae

1. Introduction

Asymptotic giant branch (AGB) stars are a significant contributor to the enrichment of galaxies with elements beyond iron (trans-iron elements, TIEs, Busso *et al.* 1999). Due to the neutron source ^{13}C, the helium (He) rich region between the hydrogen (H)- and He-burning shells provides perfect conditions for the formation of heavy elements via neutron captures on seed elements like iron (s-process). If these nucleosynthesis outcomes are transported to the stellar surface by convection, they become detectable. A possible mechanism is the final thermal pulse (FTP). Here, a final flash of the He-burning shell happens after the descent from the AGB. It can mix the entire H-rich envelope to the stellar interior resulting in a H-deficient or even H-free white dwarf (WD). This scenario can explain the detection of 16 TIEs in the photosphere of the DO-type WD RE 0503–289 (Rauch et al. submitted, Rauch *et al.* 2017). The strong enrichment of up to 100 000 times solar is due to efficient radiative levitation and, thus, does not carry any information about the abundance pattern produced by AGB nucleosynthesis. Another mechanism that mixes traces of nucleosynthesis products to the surface is the third dredge up (TDU), when the surface convection zone overshoots into the He-rich region after thermal pulses of the He-burning shell on the AGB. This process should happen for stars with initial masses above 1 $M_\odot$ (Karakas & Lugaro 2016) which translates to final WD masses of $\gtrsim 0.5\,M_\odot$ (Cummings *et al.* 2018). To constrain the s-process yields, stars in a phase before becoming a WD, i.e., before diffusion can act, need to be analyzed. For central stars of planetary nebulae (CSPNe), the stellar wind is strong enough to be chemically homogeneous and to preserve the s-process yields (Unglaub 2008).

2. Objects, observations, and model atmospheres

The two hybrid PG 1159-type CSPNe Abell 43 and NGC 7094 are known as spectroscopic twins with the same atmospheric parameters of $T_{\rm eff}$=115 kK and $\log g$=5.6

(Fig. 2). Both are H-deficient with surface H mass fractions of $25 \pm 3\,\%$ and $15 \pm 3\,\%$, respectively (Löbling *et al.* 2019b). Nucleosynthesis calculations predict the AGB s-process to be most efficient for stars with initial masses of about $3\,M_{\odot}$ which translates into post-AGB masses of $0.7 - 0.8\,M_{\odot}$. The extremely hot ($T_{\rm eff}=150$ kK, $\log g=5.7$) PG 1159-type central star of NGC 246 (Rauch & Werner 1997) falls into that region. The hot DAO-type WD BD−22°3467, the CS of Abell 35, is H-rich. Ziegler *et al.* (2012) derived a very low mass of $0.53^{+0.04}_{-0.03}\,M_{\odot}$ from interpolation of evolutionary tracks with the atmospheric parameters $T_{\rm eff}=80$ kK and $\log g=7.2$ (Fig. 2, Ziegler *et al.* 2012).

The results were obtained from analyses of high resolution spectra from ultraviolet to the optical or even infrared regime, i.e., from FUSE (910 – 1180 Å), STIS (1150 – 1730 Å) or GHRS (1140 – 1435 Å) as well as UVES (3280 – 4560 , 4580 – 6690 Å). For NGC 246, we present recent XSHOOTER (3000 – 25000 Å) spectra. To our knowledge, no optical observations of Abell 35 are available with a sufficient signal-to-noise (S/N) ratio to detect features of the hot DAO-type WD in this regime that is dominated by the cool (3700 K, Herald & Bianchi 2002) companion.

The analyses were performed using the model atmosphere code of the Tübingen NLTE Model atmosphere package (TMAP). The input atomic data for the light elements (atomic number $Z < 20$) was taken from the Tübingen Model Atom Database (TMAD, http://astro.uni-tuebingen.de/~TMAD/), for all elements with $Z \geqslant 20$, statistical atoms (Rauch & Deetjen 2003) were constructed. The atomic data for the iron group elements ($20 \leqslant Z \leqslant 28$) was taken from Kurucz's line list (http://kurucz.harvard.edu/atoms.html) and for the TIEs from the Tübingen Oscillator Strengths Service (TOSS, http://dc.g-vo.org/TOSS).

3. Selected results and their discussion

For the two hybrid PG 1159-type CSPNe Abell 43 and NGC 7094, upper abundance limits for the s-process elements could be determined (Fig. 1). Although that does not help constraining AGB yields, the fact that these upper limits lie below the strong enrichment determined in the DO-type WD RE 0503−289 (Hoyer *et al.* 2017), confirms the understanding of stellar wind and diffusion. While diffusion can accumulate s-process elements in the atmosphere of post-AGB stars in the regime of hot WDs, the strong, coupled stellar wind of CSPNe prevents this process. The abundance determination was hampered by the lack of atomic data of highly ionized (stages VIII–IX) s-process elements. This was also a reason why no reasonable upper abundance limits can be determined for s-process elements in NGC 246 (Fig. 1). Here, the problem becomes more severe due to the higher temperature. Another problem is the strong line broadening observed in its spectrum. This is consistent with a rotational velocity of 75 km/s (Löbling 2018) but could also be of different origin. While Abell 43 and NGC 7094 also show broadened lines, some PG 1159 stars, e.g. K 1 – 16, in the same $T_{\rm eff}$ –$\log g$ regime show no signatures of rotation (Werner *et al.* 2010). We speculate whether this might be connected to the finding, that NGC 246 is a pulsator (Ciardullo & Bond 1996) while K 1 – 16 does not pulsate (Sowicka *et al.* 2018).

The analysis of XSHOOTER spectra of NGC 246 reveals that the profiles of the He II $4-n$ lines with $n=6-11$ can be reproduced with a model atmosphere with $T_{\rm eff}=150$ kK and $\log g=5.7$. Using these values with the V magnitude and the mass $0.74^{+0.19}_{-0.23}\,M_{\odot}$ (Löbling 2018), we find a spectroscopic distance of 970 ± 200 pc. The distance based on Gaia parallaxes is 506 ± 25 pc (Bailer-Jones *et al.* 2018). This value would require $\log g=6.0-6.1$. A higher surface gravity is in disagreement with the He II line profiles (Fig. 3) and cannot be solved by varying the He abundance. The same phenomenon

https://doi.org/10.1017/S1743921320000617 Published online by Cambridge University Press

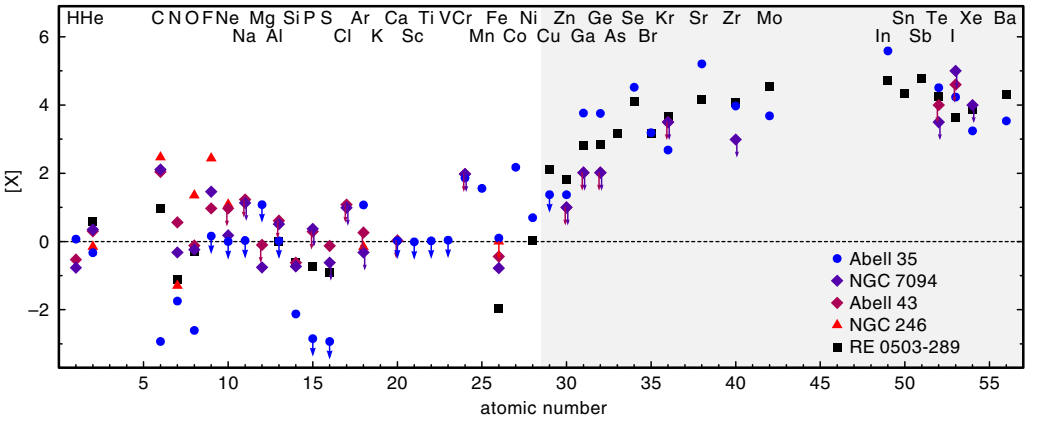

Figure 1. Abundances [X] = log (mass fraction/solar mass fraction) of the CS of Abell 35, Abell 43, NGC 7094, and NGC 246 from Löbling (2018); Löbling *et al.* (2019a,b). Upper limits are indicated with arrows. For comparison, the abundances of RE 0503–289 are shown (Hoyer *et al.* 2017).

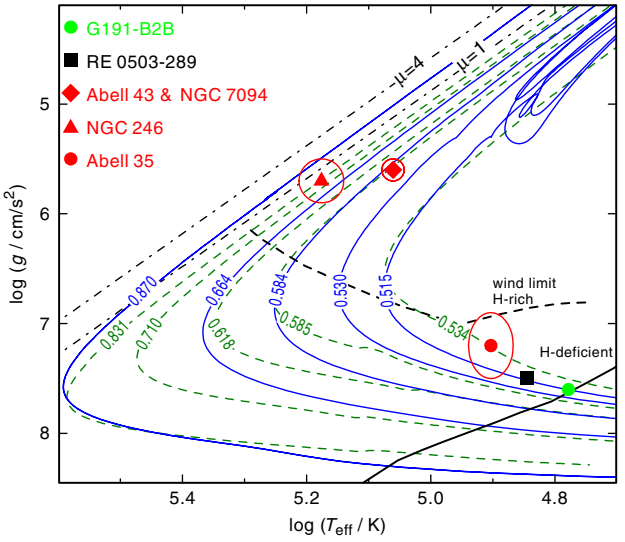

Figure 2. Location of the CS of Abell 35, Abell 43, NGC 7094, and NGC 246 (red) with error ellipses in the $T_{\rm eff}-\log g$ diagram. Included are post-AGB tracks for H-burners (green dashed, Miller Bertolami 2016) and final flashers (blue, Miller Bertolami & Althaus 2007) labeled with the stellar mass (in $M_{\odot}$). The Eddington limits for H- and He-rich atmospheres are indicated (black, dashed-dotted). The wind limit for H-rich and H-deficient post-AGB stars is indicated (Unglaub & Bues 2000).

of too high spectroscopic distances was found for other NLTE analyses (Schönberner *et al.* 2018; Schönberner & Steffen 2019). Their argument of missing metal line blanketing does not hold in our case, since opacities of 17 elements up to Ni are included in the model-grid calculations. The line profiles are calculated based on broadening tables of Schoening & Butler (1989a,b). It needs to be investigated, whether line broadening theory can cause the discrepancy. It is highly desirable to solve this tension, since a precise knowledge of $T_{\rm eff}$ and $\log g$ is required to perform reliable abundance measurements.

https://doi.org/10.1017/S1743921320000617 Published online by Cambridge University Press

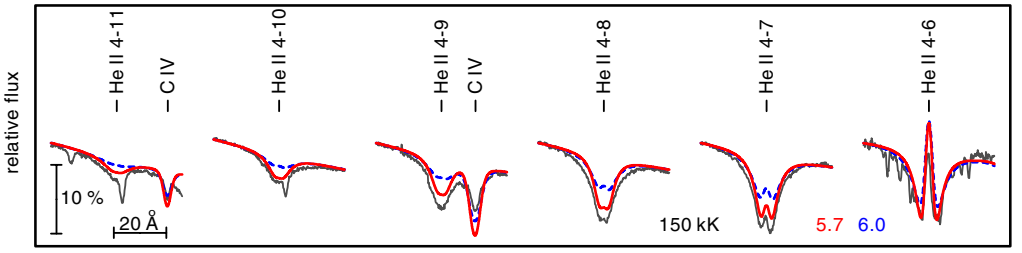

Figure 3. Synthetic spectra calculated with $T_{\rm eff}$=150 kK and log g=5.7 (red) and 6.0 (blue, dashed), compared with the He II lines in the XSHOOTER observations of NGC 246 (gray).

For the DAO-type CS of Abell 35, a high enrichment of the level of RE 0503−289 with s-process elements was found (Fig. 1). While RE 0503−289 evolved through a FTP and shows intershell material at the surface, Abell 35 still has its H-rich envelope. With its very low mass ($0.533^{+0.040}_{-0.025}\,M_{\odot}$, Ziegler *et al.* 2012), it is unclear, whether it ever experienced TDU that could pollute the atmosphere. This result raises the question, whether FTP mixing is necessary for the peculiar abundance pattern or whether it is the sole result of effective diffusion accumulating initial material.

Acknowledgement

The author would like to thank the IAU for awarding a travel grant to attend the symposium and Scot Kleinman for the careful review of this work. This research has been supported by the German Research Foundation (DFG) under grant WE 1312/49–1. The GAVO project at Tübingen had been supported by the Federal Ministry of Education and Research (BMBF) at Tübingen (05 AC 6 VTB, 05 AC 11 VTB). Based on observations collected at the European Southern Observatory under ESO programme 0102.D-0144.

References

Bailer-Jones, C. A. L. *et al.* 2018, *AJ*, 156, 58
Busso, M. *et al.* 1999, *ARA&A*, 37, 239
Ciardullo, R. & Bond, H. E. 1996, *AJ*, 111, 2332
Cummings, J. D. *et al.* 2018, *ApJ*, 866, 21
Herald, J. E. & Bianchi, L. 2002, *ApJ*, 580, 434
Hoyer, D. *et al.* 2017, *A&A*, 598, A135
Karakas, A. I. & Lugaro, M. 2016, *ApJ*, 825, 26
Löbling, L. 2018, *Galaxies*, 6, 65
Löbling, L. *et al.* 2019a, arXiv e-prints, arXiv:1911.09573
Löbling, L. *et al.* 2019b, *MNRAS*, 489, 1054
Miller Bertolami, M. M. 2016, *A&A*, 588, A25
Miller Bertolami, M. M. & Althaus, L. G. 2007, *A&A*, 470, 675
Rauch, T. & Deetjen, J. L. 2003, *ASPCS*, Vol. 288, 103
Rauch, T. *et al.* 2017, *A&A*, 606, A105
Rauch, T. & Werner, K. 1997, The Third Conference on Faint Blue Stars, L. Davis Press, 217
Schoening, T. & Butler, K. 1989a, *A&AS*, 78, 51
Schoening, T. & Butler, K. 1989b, *A&A*, 219, 326
Schönberner, D. *et al.* 2018, *A&A*, 609, A126
Schönberner, D. & Steffen, M. 2019, *A&A*, 625, A137
Sowicka, P. *et al.* 2018, *MNRAS*, 479, 2476
Unglaub, K. 2008, *A&A*, 486, 923
Unglaub, K. & Bues, I. 2000, *A&A*, 359, 1042
Werner, K. *et al.* 2010, *ApJ*, 719, L32
Ziegler, M. *et al.* 2012, *A&A*, 548, A109

https://doi.org/10.1017/S1743921320000617 Published online by Cambridge University Press